

Dielectric Elastomers for Artificial Muscles

J.-D. Nam¹, H.R. Choi², J.C. Koo², Y.K. Lee³, K.J. Kim⁴

¹ Department of Polymer Science and Engineering, Sungkyunkwan University, 300 Chunchun-dong, Jangan-gu, Suwon, Kyunggi-do 440-746, South Korea, dnam@skku.edu

² School of Mechanical Engineering, Sungkyunkwan University, 300 Chunchun-dong, Jangan-gu, Suwon, Kyunggi-do 440-746, South Korea

³ School of Chemical Engineering, Sungkyunkwan University, 300 Chunchun-dong, Jangan-gu, Suwon, Kyunggi-do 440-746, South Korea

⁴ Active Materials and Processing Laboratory, Mechanical Engineering Department (MS312), University of Nevada, Reno, NV 89557, USA

2.1 Introduction

Natural muscles have self-repair capability providing billions of work cycles with more than 20% of contractions, contraction speed of 50% per second, stresses of ~0.35 MPa, and adjustable strength and stiffness [1]. Artificial muscles have been sought for artificial hearts, artificial limbs, humanoid robots, and air vehicles. Various artificial muscles have been investigated for large strain, high response rate, and high output power at low strain using their own material characteristics [2]. Among the candidates for artificial muscles, the dielectric elastomer has typical characteristics of light weight, flexibility, low cost, easy fabrication, *etc.*, which make it attractive in many applications. Applications of dielectric elastomer include artificial muscles and also mobile robots, micro-pumps, micro-valves, disk drives, flat panel speakers, intelligent endoscope, *etc.* [3–7].

Dielectric elastomer actuators have been known for their unique properties of large elongation strain of 120–380%, large stresses of 3.2 MPa, high specific elastic energy density of 3.4 J/g, high speed of response in 10^{-3} s, and high peak strain rate of 34,000%/sec [1,2,4,8]. They transform electric energy directly into mechanical work and produce large strains. Their actuators are composed primarily of a thin passive elastomer film with two compliant electrodes on the surfaces, exhibiting a typical capacitor configuration. As with most rubbery materials, the elastomer used in actuator application is incompressible (Poisson's ratio = 0.5) and viscoelastic, which consequently exhibits time- or frequency-dependent characteristics that could be represented by stress relaxation, creep, and dynamic-mechanical phenomena under stressed and deformed states [9–10]. When the electrical voltage is applied to the electrodes, an electrostatic force is generated between the electrodes. The force is compressive, and thus the elastomer film expands in the in-plane direction.

As an advantage of dielectric elastomer actuators, the performance of elastomer actuators can be tailored by choosing different types of elastomers, changing the cross-linking chemistry of polymer chains, adding functional entities, and improving fabrication techniques with ease and versatility in most cases. The deformation of elastomers complies with the theories of rubber elasticity and nonlinear viscoelasticity. When an electrical field is applied, the elastomer deformation is influenced primarily by the intrinsic properties of moduli and dielectric constants of elastomers in a coupled manner. In addition, maximum actuation capabilities are often restricted by the dielectric strength (or breakdown voltage) of elastomer films. Although the low stiffness of elastomers may increase strain, maximum actuator stroke, and work per cycle, it should be considered that the maximum stress generation decreases with decreased moduli. Accordingly, the property-processing-structure relationship of elastomers especially under the electrical field and large deformation should be understood on the basis of the fundamental principles of deforming elastomers and practical experience in actuator fabrication.

2.2 General Aspects of Elastomer Deformation

Elastomers can be stretched several hundred percent; yet on being released, they contract back to their original dimensions at high speeds. By contrast, metals, ceramics, or other polymers (linear or highly cross-linked polymers) can be stretched reversibly for only about 1%. Above this level, they undergo permanent deformation in an irreversible way and ultimately break. This large and reversible elastic deformation makes elastomers unique in actuator applications. The fundamental dielectric and mechanical properties of most common elastomers are summarized in Table 2.1.

Elastomers are lightly-crosslinked polymers. Without cross-linking, the polymer chains have no chemical bonds between chains, and thus the polymer may flow upon heating over the glass transition temperature. If the polymer is densely cross-linked, the chains cannot flow upon heating, and a large deformation cannot be expected upon stretching. Elastomers are between these two states of molecular conformation. The primary chains of elastomers are cross-linked at some points along the main polymer chains. For example, commercial rubber bands or tires have molecular weights of the order of 10^5 g/mol and are cross-linked every $5\text{--}10 \times 10^3$ g/mol, which gives 10–20 cross-links per primary polymer molecule. The average molecular weight between cross-links is often defined as M_c to express degree of cross-linkage.

A raw elastomer is a high molecular weight liquid with low strength. Although its chains are entangled, they readily disentangle upon stressing and finally fracture in viscous flow. Vulcanization or curing is the process where the chains of the raw elastomer are chemically linked together to form a network, subsequently transforming the elastomeric liquid to an elastic solid. The most widely used vulcanizing agent is sulfur that is commonly used for diene elastomers such as butadiene rubber (BR), styrene-butadiene rubber (SBR), acrylonitrile-butadiene rubber (NBR), and butyl rubber (IIR). Another type of curing agent is peroxides,

which are used for saturated elastomers such as ethylene propylene rubber, chlorinated polyethylene (CSM), and silicone elastomers. The mechanical behavior of an elastomer depends strongly on cross-link density. When an uncross-linked elastomer is stressed, chains may readily slide past one another and disentangle. As cross-linking is increased further, the gel point is eventually reached, where a complete three-dimensional network is formed, by definition. A gel cannot be fractured without breaking chemical bonds. Therefore, the strength is higher at the gel point, but it does not increase indefinitely with more cross-linking. The schematic of elastomer properties is shown as a function of cross-link density in Figure 2.1. The elastomer properties, especially the modulus, are significantly changed by the cross-link density in most elastomer systems, and thus the actuator performance can be adjusted by controlling the degree of elastomer vulcanization (degree of cross-link density). The cross-link density can be adjusted by the kinetic variables of vulcanization reactions such as sulfur (or peroxide) content, reaction time, reaction temperature, catalyst (or accelerator), *etc.* Note that the elastomer vulcanization process is not a thermodynamic process but a kinetically-controlled process in most cases.

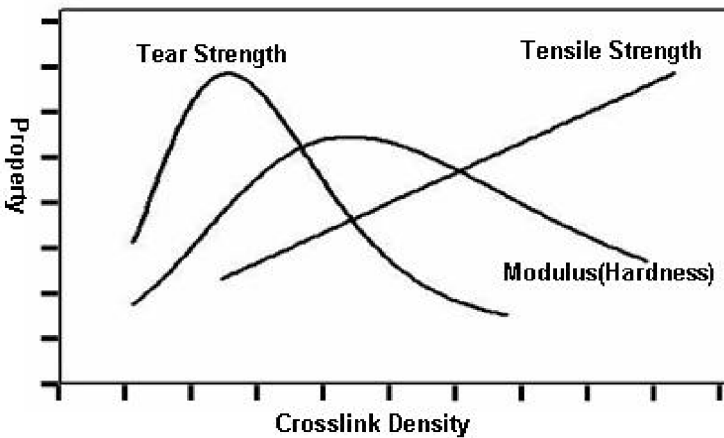
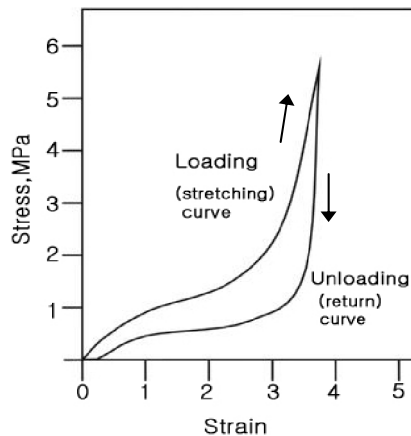


Figure 2.1. Elastomer properties schematically plotted as a function of cross-link density

Another significant phenomena in elastomers is the hysteresis loop of stress-strain curves. As seen in Figure 2.2, the stress under loading and unloading is different in the pathway. Furthermore, the unloading curve usually does not return to the origin. As the elastomer is allowed to rest in a stress-free state, the strain will reach the origin. It should also be mentioned that the shape of the hysteresis loop changes with loading-unloading cycles, especially in the early stage of cycles, eventually reaching an identical hysteresis loop. The hysteresis phenomena of elastomers should be considered in the development of actuators for long-term durability.

Table 2.1. Dielectric and mechanical properties of elastomers [11, 12]

	Dielectric constant at 1kHz	Dielectric loss factor at 1kHz	Young's modulus [$\times 10^6$ Pa]	Eng. stress [MPa]	Break stress [MPa]	Ultimate strain [%]
Polyisoprene, natural rubber(IR)	2.68	0.002–0.04	1.3	15.4	30.7	470
Poly(chloroprene)(CR)	6.5–8.1	0.03/0.86	1.6	20.3	22.9	350
Poly(butadiene)(BR)	–	–	1.3	8.4	18.6	610
Poly(isobutene–co–isoprene)butyl rubber	2.42	0.0054	1	–	17.23	–
Poly(butadiene–co–acrylonitrile)(NBR, 30% acrylonitrile constant)	5.5 (10^6 Hz)	35 (10^6 Hz)		16.2	22.1	440
Poly(butadiene–co–styrene) (SBR, 25% styrene constant)	2.66	0.0009	1.6	17.9	22.1	440
Poly(isobutyl–co–isoprene rubber)(IIR)	2.1–2.4	0.003	–	5.5	15.7	650
Chlorosulfonated polyethylene(CSM)	7–10	0.03–0.07	–	–	24.13	–
Ethylene–propylene rubber(EPR)	3.17–3.34	0.0066–0.0079	–	–	20.68	–
Ethylene–propylene diene monomer (EPDM)	3.0–3.5	0.0004 at 60 Hz	2	7.6	18.1	420
Urethane	5–8	0.015–0.09	–	–	20–55	–
Silicone	3.0–3.5	0.001–0.010	–	–	2–10	80–500

**Figure 2.2.** Stress-strain curve of elastomers under loading and unloading a exhibiting hysteresis loop

2.3 Elastic Deformation of Elastomer Actuator under Electric Fields

The electrostatic energy (U) stored in an elastomer film with thickness z and surface area A can be written as

$$U = \frac{Q^2}{2C} = \frac{Q^2 z}{2\epsilon_o \epsilon_r A} \quad (2.1)$$

where Q , C , ϵ_o , and ϵ_r are the electrical charge, capacitance, free-space permittivity (8.85×10^{-12} F/m), and relative permittivity, respectively. The capacitance is defined as $C = \epsilon_o \epsilon_r A / z$. From the above equation, the change in electrostatic energy can be related to the differential changes in thickness (dz) and area (dA) with a constraint that the total volume is constant ($Az = \text{constant}$). Then the electrostatic pressure generated by the actuator can be derived as [5]

$$P = \epsilon_o \epsilon_r E^2 = \epsilon_o \epsilon_r \left(\frac{V}{z} \right)^2 \quad (2.2)$$

where E and V are the applied electric field and voltage, respectively. The electrostatic pressure in Eq. (2.2) is twofold larger than the pressure in a parallel-plate capacitor due to that fact that the energy would change with the changes in both the thickness and area of actuator systems.

Actuator performance has been derived by combining Eq. (2.2) and a constitutive equation of elastomers. The simplest and the most common equation of state may combine Hooke's law with Young's modulus (Y), which relates the stress (or electrostatic pressure) to thickness strain (s_z) as

$$P = -Ys_z \quad (2.3)$$

where $z = z_o(1 + s_z)$ and z_o is the initial thickness of the elastomer film. Using the same constraint that the volume of the elastomer is conserved, $(1 + s_z)(1 + s_x)(1 + s_y) = 1$ and $s_x = s_y$, the in-plane strain (s_x or s_y) can be derived from Eqs. (2.2) and (2.3). For example, when the strain is small (e.g., less than 20%), which may be not the case in practical actuator application, z in Eq. (2.2) can be simply replaced by z_o , and the resulting equation becomes

$$s_z = -\frac{\epsilon_o \epsilon_r}{Y} \left(\frac{V}{z_o} \right)^2 \quad (2.4)$$

or the in-plane strain can be expressed because $s_x = -0.5s_z$,

$$s_x = -\frac{\varepsilon_o \varepsilon_r}{2Y} \left(\frac{V}{z_o} \right)^2 \quad (2.5)$$

This equation often appears in published literature. When the strain is large, however, the strain should be derived by combining Eqs. (2.2) and (2.3) in a quadratic equation:

$$s_z = -\frac{2}{3} + \frac{1}{3} \left[f(s_o) + \frac{1}{f(s_o)} \right] \quad (2.6)$$

where $f(s_o) = \left[1 + 13.5s_o + \sqrt{27s_o(6.75s_o - 1)} \right]^{1/3}$ and $s_o = -\frac{\varepsilon_o \varepsilon_r}{Y} \left(\frac{V}{z_o} \right)^2$

The through-thickness strain s_z can be converted to in-plane strain by solving the quadratic equation for the strain constraint as

$$s_x = (1 + s_z)^{-0.5} - 1 \quad (2.7)$$

For low strain materials, the elastic strain energy density (u_e) of actuator materials has been estimated as [4]

$$u_e = \frac{1}{2} P s_z = \frac{1}{2} Y s_z^2 \quad (2.8)$$

However, for high strain materials, the in-plane area over which the compression is applied changes markedly as the material is compressed, and thus the elastic strain energy density can be obtained by integrating the compressive stress times the varying planar area over the displacement, resulting in the following relation [4]:

$$u_e = \frac{1}{2} P \ln(1 + s_z) \quad (2.9)$$

However, it should be mentioned that Eqs. (2.4) and (2.6) are based on Hooke's equation of state, which may not be applicable to all elastomer systems. Elastomers usually have nonlinear and viscoelastic behavior in stress-strain relations, and thus the performance of the elastomer actuator should be analyzed by using a more realistic equation of state based on the fundamental theory and modeling methodology of rubber elasticity.

2.4 Rubber Elasticity and Equation of State of Elastomers

The relationships among macroscopic deformation, microscopic chain extension, and entropy reduction have been derived by many researchers providing quantitative relations between chain extension and entropy reduction [9,11,13,14]. The fundamental principle is that the repulsive stress of an elastomer arises from the reduction of the entropy of elastomers rather than through changes in enthalpy. As a result, the basic equation between stress and deformation is given as (for unidirectional compression and expansion)

$$P = -nRT \left(\lambda - \frac{1}{\lambda^2} \right) \quad (2.10)$$

where R is gas constant, T is temperature, and λ is the ratio of length (L) to the original length (L_o), *i.e.*, $\lambda = L/L_o$, and thus it is related to the thickness strain in Eq. (2.3) as $\lambda = 1 + s_z$. The quantity n represents the number of active network chain segments per unit volume [15, 16]. It should be mentioned that the extension (or contraction) ratio is usually used in the description of deformation in elastomer systems instead of strain because the extent of deformation is relatively large. The quantity n represents the number of active network chain segments per unit volume, which is equal to ρ/M_c , where ρ and M_c are the density and the molecular weight between cross-links. As can be seen in Eq. (2.8), the equation is nonlinear and consequently the Hookean relation does not hold. However, Eq. (2.10) is often valid for relatively small extensions in most elastomers. The actual behavior of cross-linked elastomers in unidirectional extension is well described by the empirical equation of Mooney-Rivlin [17]:

$$P = - \left(C_1 + \frac{C_2}{\lambda} \right) \left(\lambda - \frac{1}{\lambda^2} \right) \quad (2.11)$$

According to the above equation, a plot of $P/(\lambda - 1/\lambda^2)$ versus $1/\lambda$ should be linear especially at low elongation, where C_1 and C_2 are obtained from the slope and intercept of the plot. The value of $C_1 + C_2$ is nearly equal to the shear modulus (or $Y/3$). Table 2.2 summarizes typical values of C_1 and C_2 of several elastomers.

2.5 Nonlinear Viscoelasticity of Elastomers in Creep and Stress Relaxation

For the application of elastomer actuators, the prestrain condition (~50–100%) is a substantial factor in actuator design and application. The prestrained condition of elastomers can be suited to nonlinear viscoelastic creep or stress relaxation characteristics in a large deformation. Various theories and models have been

developed to analyze the nonlinear viscoelastic behavior of polymers in a large strain [9,10,13]. Here, we will introduce several methods applicable to the development and analysis of elastomer actuators under prestrained or actuating conditions.

Table 2.2. Constants of the Mooney-Rivlin equation [14]

Elastomer	C_1	C_2	$(C_1 + C_2)$	$C_2 / C_1 + C_2$
Natural	2.0(0.9–3.8)	1.5(0.9–2)	3.5	0.4(0.25–0.6)
Butyl rubber	2.6(2.1–3.2)	1.5(1.4–1.6)	4.1	0.4(0.3–0.5)
Styrene–butadiene rubber	1.8(0.8–2.8)	1.1(1.0–1.2)	2.9	0.4(0.3–0.5)
Ethane–propene rubber	2.6(2.1–3.1)	2.5(2.2–2.9)	5.1	0.5(0.43–0.55)
Polycrylate rubber	1.2(0.6–1.6)	2.8(0.9–4.8)	3	0.5(0.3–0.8)
Silicone rubber	0.75(0.3–1.2)	0.75(0.3–1.1)	1.5	0.4(0.25–0.5)
Polyurethane	3(2.4–3.4)	2(1.8–2.2)	5	0.4(0.38–0.43)

To describe the creep behavior of elastomers with a large deformation ($\sim 100\%$), separable stress and time functions have been proposed. The model proposed by Pao and Marin is based on the assumption that the total creep strain is composed of an elastic strain, transient recoverable viscoelastic strain, and a permanent non-recoverable strain [18]:

$$s(t) = P/Y + KP^n (1 - s^{-qt}) + BP^n t \quad (2.12)$$

where K , n , q and B are constants for the material.

Findley *et al.* have fitted the creep behavior of many polymers to the following analytical relation in a form of power-law equation [19]:

$$s(t) = s_o + mt^n \quad (2.13)$$

where s_o and m are functions of stress for a given material and n is a material constant. A more general relation for the single-step loading tests can be written as [9]

$$s(P, t) = s_o \sinh \frac{P}{P_o} + mt^n \sinh \frac{P}{P_m} \quad (2.14)$$

where m , P_o , and P_m are constants for a material.

A similar relationship has been proposed by Van Holde [20]:

$$s(t) = s_o + mt^{1/3} \sin \alpha P \quad (2.15)$$

where α is a constant.

When a constant strain is applied to the elastomer actuators as a prestrain, the stress changes as a function of time and prestrain values. The nonlinear stress relaxation behavior with a large strain has taken a rheological approach. For example, the model proposed by Martin *et al.* is as follows [9];

$$P = Y \frac{s}{\lambda^2} \exp A \left(\lambda - \frac{1}{\lambda} \right) \quad (2.16)$$

where λ is the extension ratio and A is a constant.

2.6 Tunable Properties of Dielectric Constant and Modulus of Elastomers

According to Eq. (2.5), actuator performance is directly influenced by the stiffness and dielectric constant of an elastomer. In terms of actuator strain, lower values of the modulus and higher values of the dielectric constant are desirable. However, in terms of stress, the lower modulus values are not always desirable because the maximum stress attainable from an actuator increases with the modulus of elastomers. Accordingly, the dielectric constant and modulus should be optimized to give the desired performance of dielectric elastomer actuators.

The dielectric constant of elastomers can be enhanced simply by incorporating high dielectric materials. For example, copper phthalocyanine oligomere (CPO) has been blended with silicones to increase dielectric constants [2,21,22]. In this approach, the dielectric constant increased from 3.3 to 11.8 from the pristine silicone to a silicone blend with 40 wt% of CPO, which corresponds to a 250% increment in the dielectric constant. As discussed in Eqs. (2.4) and (2.5), the increased dielectric constant provides increased strain of the elastomer actuator [3]. However, it should be mentioned that the dielectric strength (or breakdown voltage) of an elastomer film is one of the most substantial factors in actuator applications. Incorporating heterogeneous entities or ionic chemicals usually decreases the dielectric strength, and subsequently the actuator performance should be limited by the applicable electric fields. Although the strain of the CPO/silicone blend system is increased, the maximum attainable strain is decreased by a deteriorated breakdown voltage [3].

It has also been reported that the gallery height of montmorillonite (MMT), a layered inorganic clay nanoplatelet system forms distributed effective nanocapacitors when incorporated in polymers [23]. The resulting dielectric constant and ionic conductivity have increased by 20–4300% and two to three orders of magnitude, respectively, in phenolic resin/MMT nanocomposite systems without a significant decrease in breakdown voltage. A similar nanocapacitance effect has been observed in polyurethane elastomer/MMT nanocomposite systems exhibiting an increment in dielectric constant from 2.6 to 5.6 [24]. It should be mentioned that the morphology of the layered nanoplatelets determines the dielectric constant as well as the modulus of nanocomposite systems. When

nanoplatelets are homogeneously dispersed (or exfoliated) in a polymer, the modulus is significantly increased with a slight increment in the dielectric constant. On the other hand, when the polymer is intercalated between nanoplatelets, the modulus is not much increased but the dielectric constant is increased [24].

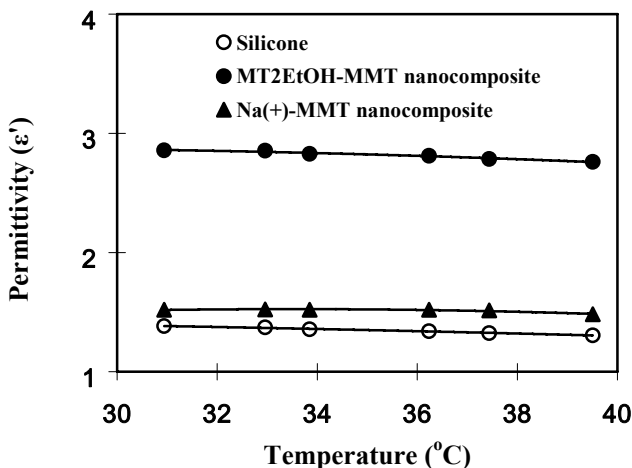


Figure 2.3. Dielectric constants of pristine silicone elastomer compared with its nanocomposite systems containing Na⁺ ion and MT2EtOH as intercalants in MMT

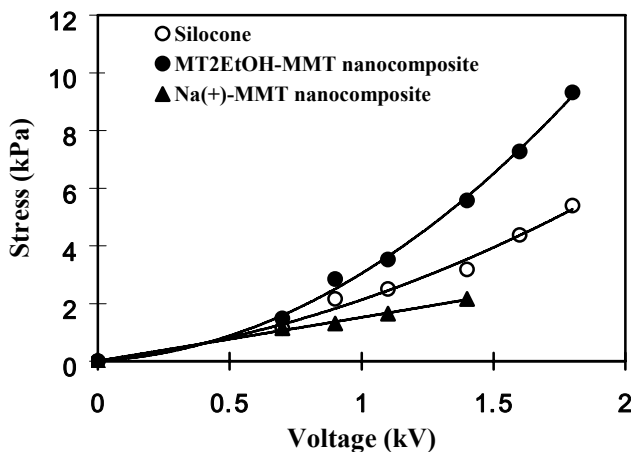


Figure 2.4. Comparison of electric-field-induced stress for pristine silicone and two nanocomposite systems measured up to breakdown voltages

In Figure 2.3, for example, the dielectric constant of a silicone-based polymer is compared with two nanocomposite systems containing two different types of

commercial montmorillonite systems (Southern Clay Production): Na⁺/MMT and 92.6 meq/100 g ($d_{001}=11.7\text{\AA}$), and methyl tallow bis-2-hydroxyethylammonium (MT2EtOH)/MMT 90 meq/100 g ($d_{001}=18.5\text{\AA}$), where tallow is predominantly composed of octadecyl chains with small amounts of low homologues (~65% of C₁₈, ~30% of C₁₆ and ~5% of C₁₄). The layer thickness of an MMT sheet is around 1 nm and the lateral dimensions vary from several nanometers to micrometers. The Na⁺/MMT system gives an exfoliated or isotropically dispersed state of nanoplatelets, and the MT2EtOH/MMT system gives an intercalated structure maintaining the layered structure of MMT platelets. As with the urethane elastomer system, the intercalated MMT/silicone nanocomposite provides a higher dielectric constant than the exfoliated system seemingly due to the nanocapacitance effect. The well-known fact that the exfoliated nanocomposites give the highest modulus value is also demonstrated in these silicone nanocomposite elastomer systems; 55 kPa for silicone, 88 kPa for a Na⁺-MMT nanocomposite, and 72 kPa for a MT2EtOH-MMT nanocomposite.

For these three systems of silicone-based materials, the generated stress is compared in Figure 2.4. As can be seen, the intercalated MT2EtOH-MMT actuator provides the highest stress values generated in the whole range of the electric field up to the breakdown voltage. It is due to the increased dielectric constant induced by the layered nanocapacitance effect. It should be pointed out that the breakdown voltage of the nanocomposite system is not decreased by the incorporation of nanoplatelets, which can hardly be achieved in other chemicals or fillers.

2.7 References

- [1] R.H. Baughman, *Science* 308, 63 (2005).
- [2] Y. Bar-Cohen, *Electroactive Polymer (EAP) Actuators as Artificial Muscles-Reality, Potential and Challenges*, Vol. PM136, SPIE-Society of Photo-optical Instrumentation Engineers, Bellingham, WA 2004.
- [3] X. Zhang, C. Löwe, M. Wissler, B. Jähne, and G. Kovacs, *Advanced Engineering Materials*, 7(5), 361 (2005).
- [4] R. Pelrine, R. Kornbluh, Q. Pei, J. Joseph, *Science*, 287, 836 (2000).
- [5] R. Pelrine, R. Kornbluh, J.P. Jeseoph, *Sensors and Actuators A64*, 77 (1999).
- [6] H.R. Choi, K.M. Jung, J.C. Koo, J.D. Nam, Y.K. Lee, and M.S. Cho, *Key Engineering Materials*, 297-300, 622 (2005).
- [7] J.C. Koo, H.R. Choi, M.Y. Jung, K.M. Jung, J.D. Nam, Y.K. Lee, *Key Engineering Materials*, 297-300, 665 (2005).
- [8] J.D. Madden, *IEEE Journal of Oceanic Engineering*, 29, 706 (2004).
- [9] I.M. Ward, *Mechanical Properties of Solid Polymers*, John Wiley & Sons, New York, (1985).
- [10] J. D. Ferry, *Viscoelastic Properties of Polymers*, John Wiley & Sons, New York, (1980).
- [11] A.N. Gent (ed.), *Engineering with Rubber*, Hanser, New York (1992).
- [12] J. Brandrup, E.H. Immergut, E. A. Grulke (eds.), *Polymer Handbook*, 4th Ed., John Wiley & Sons, New York (1999).
- [13] L. Nielsen and R.F. Landel, *Mechanical Properties of Polymers and Composites*, Marcel Dekker, New York (1994).
- [14] D.W. Van Krevelen, *Properties of Polymers*, Elsevier, New York (1990).

- [15] P.J. Flory, *Polymer*, 20, 1317 (1979).
- [16] L.R.G. Treloar, *The Physics of Rubber Elasticity*, 3rd ed., Clarendon Press, Oxford, (1975).
- [17] M. Mooney, *Journal of Applied Physics*, 11, 582 (1940); M. Mooney, *Journal of Applied Physics*, 19, 434 (1948); R.S. Rivlin, *Transactions of the Royal Society (London)*, A240, 459, 491, 509 (1948); R.S. Rivlin, *Transactions of the Royal Society (London)*, A241, 379 (1948).
- [18] T.H. Pao and J. Martin, *Journal of Applied Mechanics*, 19, 478 (1952); *Journal of Applied Mechanics*, 20, 245 (1953).
- [19] W.N. Findley and G. Khosla, *Journal of Applied Physics*, 26, 821 (1955).
- [20] R. Van Holde, *J. Polym. Sci.*, 24, 417 (1957).
- [21] Q.M. Zhang, H. Li, M. Poh, F. Xia, Z.-Y. Cheng, H. Xu, C. Huang, *Nature*, 419, 284 (2002).
- [22] B. Achar, G. Fohlen, J. Parker, *Journal of Polymer Science Part A: Polymer Chemistry*, 20, 1785 (1982).
- [23] E.P.M. Williams, J.C. Seferis, C.L. Wittman, G.A. Parker, J.H. Lee, J.D. Nam, *Journal of Polymer Science Part A: Polymer Physics*, 42, 1-4 (2004).
- [24] J.-D. Nam, S. D. Hwang, H. R. Choi, J. H. Lee, K. J. Kim, and S. Heo, *Smart Materials and Structures*, 14, 87-90 (2004).



<http://www.springer.com/978-1-84628-371-0>

Electroactive Polymers for Robotic Applications

Artificial Muscles and Sensors

Kim, K.J.; Tadokoro, S. (Eds.)

2007, X, 281 p., Hardcover

ISBN: 978-1-84628-371-0